Resource

Cell Chemical Biology

# Linkage-Specific Detection and Metabolism of Human Milk Oligosaccharides in *Escherichia coli*

## Graphical Abstract

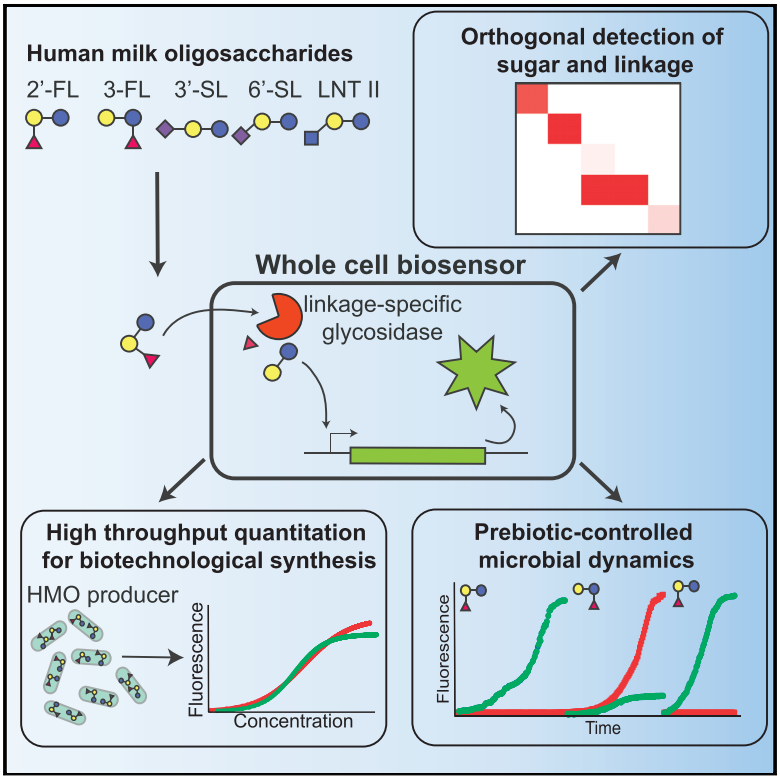


## Highlights

- Linkage-specific, orthogonal detection of five abundant human milk oligosaccharides
- Selective utilization of HMOs enabling growth-based selection
- Robust against crosstalk allowing parallel sensing
- Dynamic regulation of growth and protein production in mixed cultures

## Authors

Fatima Enam, Thomas J. Mansell

## Correspondence

mansell@iastate.edu

## In Brief

Quantitation and glycoside linkage analysis of complex sugars often requires chromatography and/or mass spectrometry. Enam and Mansell have devised a biosensor that enables high-throughput, linkage-specific detection of human milk oligosaccharides and enables dynamic regulation of growth and protein expression in mixed cultures.

Enam & Mansell, 2018, Cell Chemical Biology *25*, 1–12
September 20, 2018 
https://doi.org/10.1016/j.chembiol.2018.06.002

CellPress

Please cite this article in press as: Enam and Mansell, Linkage-Specific Detection and Metabolism of Human Milk Oligosaccharides in *Escherichia coli*, Cell Chemical Biology (2018), https://doi.org/10.1016/j.chembiol.2018.06.002

Cell Chemical Biology
Resource

# Linkage-Specific Detection and Metabolism of Human Milk Oligosaccharides in *Escherichia coli*

Fatima Enam[1] and Thomas J. Mansell[1,2,*]
[1]Department of Chemical and Biological Engineering, Iowa State University, Ames, IA 50011, USA
[2]Lead Contact
*Correspondence: mansell@iastate.edu
https://doi.org/10.1016/j.chembiol.2018.06.002

## SUMMARY

**Human milk oligosaccharides (HMOs) are important prebiotic complex carbohydrates with demonstrated beneficial effects on the microbiota of neonates. However, optimization of their biotechnological synthesis is limited by the relatively low throughput of monosaccharide and linkage analysis. To enable high-throughput screening of HMO structures, we constructed a whole-cell biosensor that uses heterologous expression of glycosidases to generate linkage-specific, quantitative fluorescent readout for a range of HMOs at detection limits down to 20 μM in approximately 6 hr. We also demonstrate the use of this system for orthogonal control of growth rate or protein expression of particular strains in mixed populations. This work enables rapid non-chromatographic linkage analysis and lays the groundwork for the application of directed evolution to biosynthesis of complex carbohydrates as well as the prebiotic manipulation of population dynamics in natural and engineered microbial communities.**

## INTRODUCTION

Human milk is the initial sole source of nutrition for many infants. In addition to its nutritive protein, fat, and carbohydrate content, it is highly abundant in unique oligosaccharides that comprise 5–15 g/L (Baumgärtner et al., 2014) or 20% of its carbohydrate content (Newburg and Neubauer, 1995). These human milk oligosaccharides (HMOs) are indigestible by the infant but play many roles in the infant gut. For example, gut bacteria capable of cleaving glycosidic linkages (Charbonneau et al., 2016; Garrido et al., 2016) can facilitate metabolism of these carbohydrates into organic acids such as butyrate, which lowers the intestinal pH and provides an important energy source for colonocytes (Kunz et al., 2000). In addition, HMOs bind pathogens by acting as decoys and inhibit adhesion to the intestinal epithelial surface, protecting breast-fed infants against diarrhea-causing pathogens (Angeloni et al., 2005; Crane et al., 1994; Newburg et al., 2004; Yu et al., 2016). HMOs have recently been shown to affect infant body mass (Alderete et al., 2015), *Candida albicans* invasion in the infant gut (Gonia et al., 2015), attenuation of inflammation in the intestine (Newburg et al., 2015), and the overall microbial makeup in the gut environment (Wang et al., 2015). Given the interesting benefits that these oligosaccharides confer on infants, especially preterm (Underwood et al., 2015), a plentiful and inexpensive supply of these carbohydrates would be of great benefit to neonatal health. However, the nature of sugars, especially the prevalence of multiple hydroxyl groups, makes synthesis of these compounds difficult.

HMOs typically have a degree of polymerization from 3 to 10 monosaccharides with a lactose (Gal-β-1,4-Glc) core at the reducing end. They are generally modified by the addition of fucose (α-1,2-, α-1,3-, or α-1,4-Fuc), sialic acid (*N*-acetylneuraminic acid) (α-2,3- or α-2,6-Sia), or glycosidic linkages (β-1,3- or β-1,6-) to other lactose or *N*-acetyllactosamine precursors. The most abundant HMOs are 2′-fucosyllactose, 3-fucosyllactose, lacto-n-fucopentaose I, and, 3′-sialyllactose (Chaturvedi et al., 2001; Coppa et al., 1999; Thurl et al., 2010). Examples of some HMO trisaccharides are shown in Figure 1A.

Various chemical and chemoenzymatic synthesis methods of HMOs have been reported (La Ferla et al., 2002; Plante et al., 2001; Prudden et al., 2017; Sears and Wong, 2001; Xiao et al., 2016; Zhao et al., 2016). However, these approaches often require rigorous protection-deprotection schemes or purified components such as activated nucleotide sugars and robust enzymes, both of which can be rather expensive to produce. Because of these limitations, biotechnological approaches for *in vivo* production of HMOs in microbes has garnered attention owing to its scalability and cost effectiveness (Petschacher and Nidetzky, 2016).

Metabolic engineering of microbial strains has been used to produce complex carbohydrates *in vivo* (Chen, 2015). Successful examples of this approach are the production of various HMOs (Baumgärtner et al., 2013; Han et al., 2012), blood groups (Drouillard et al., 2006), eukaryotic *N*-glycans (Hamilton et al., 2006; Schwarz et al., 2010; Valderrama-Rincon et al., 2012), and pathogen-mimicking glycans (Chen et al., 2016; Mally et al., 2013; Valentine et al., 2016). While metabolic engineering in microbes (Baumgärtner et al., 2013, 2014; Dumon et al., 2006; Lee et al., 2012) has shown promise, optimization of glycan production is limited by the low throughput of detection. These glycan structures can be extremely diverse because glycosidic bonds between monosaccharides can form at many different points on the sugar, leading to branching based on glycosidic linkage, and identifying these linkages is not straightforward, especially α- or β-anomeric configuration. Linkage analysis methods include nuclear magnetic resonance (van den Berg et al., 1994; Chai et al., 2005), mass spectrometric methods (reviewed in Kailemia et al., 2014), or profiling of enzyme digests,

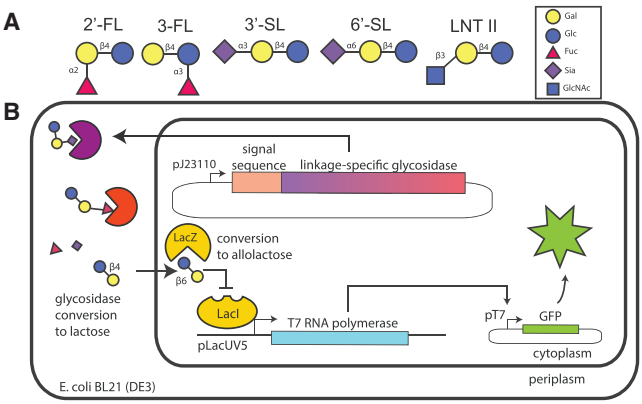


**Figure 1. Schematic of Biosensor Design**

(A) Human milk trisaccharides for which biosensors were built. From left to right: 2′-fucosyllactose (2′-FL), 3-fucosyllactose (3-FL), 3′-sialyllactose (3′-SL), 6′-sialyllactose (6′-SL), lacto-*N*-triose II (LNT II).

(B) Trisaccharides enter the bacterial periplasm and are converted to lactose by heterologous glycosidases. Lactose is transported to the cytoplasm and converted to allolactose, which activates the LacUV5 promoter in *E. coli* BL21 (DE3), producing T7 RNAP, which transcribes GFP under the T7 promoter, leading to fluorescent protein expression.

which leverages the specific affinity of enzymes for particular sugars and linkages, breaking down the glycan followed by a chromatography step for quantification (Rudd et al., 1997). An even more coarse-grained method of detecting sugar composition is acid hydrolysis of glycans with trifluoroacetic acid followed by quantitation by liquid chromatography-mass spectrometry (LC-MS) (Royle, 2013). More recently, high-pH anion-exchange chromatography (Shen et al., 2000; Suzuki and Suzuki, 2001), polysaccharide analysis by carbohydrate gel electrophoresis (Goubet et al., 2002), and capillary electrophoresis with laser-induced fluorescence (Evangelista et al., 1995) have become well established. While recent interest in glycomics has led to improvements in throughput of chromatographic/MS methods (Shubhakar et al., 2015), their maximum throughput is on the order of hundreds of samples per day without automation (Doherty et al., 2013). In addition, they also often require specialized equipment and expertise in analysis as well as sample derivatization. Substantially increased throughput of detection of these glycan moieties and linkages would enable approaches such as directed evolution (Abatemarco et al., 2013; Kuchner and Arnold, 1997; Packer and Liu, 2015) toward improved production of glycans.

In the synthetic biology community, engineering of genetic circuits has generated cellular devices that can sense and translate to a quantifiable biological response, with practical applications in biosensing, therapeutics, and production of small molecules and biofuels (Khalil and Collins, 2010; Kobayashi et al., 2004). Bacterial biosensors have been successfully developed for the detection of toxic chemicals, pollutants, drugs, and antibiotics (Green et al., 2014; Harms et al., 2006; Leveau and Lindow, 2002; van der Meer and Belkin, 2010; Paige et al., 2012; Paton et al., 2009; Strack et al., 2014; Daunert et al., 2000; Trang et al., 2005).

Here, we present the construction of a synthetic *in vivo* genetic circuit that can serve as a platform for detecting trisaccharide lactose-based HMOs. In brief, the method uses heterologous expression of glycosidases highly specific to human milk oligosaccharide carbohydrate linkages to generate lactose, the presence of which is detected by the *lac* operon. We demonstrate non-chromatographic, linkage-specific, sensitive, and orthogonal detection of five of the most abundant trisaccharide HMOs using this engineered *Escherichia coli* biosensor. We also show that HMOs can be quantitatively detected in the context of biotechnological production. In addition, we show that our engineered cells can utilize HMOs as sole carbon sources, mimicking their prebiotic effect and serving as a growth-based selection. We also demonstrate that crosstalk between strains expressing different glycosidases is minimal, demonstrating the capacity to detect distinct HMOs in parallel. Finally, we demonstrate the regulation of growth and protein expression of engineered strains in mixed culture using HMOs as inducers. Taken in total, this work represents a robust system for massively parallel optimization of biotechnological production of human milk oligosaccharides and HMO-based dynamic regulation of growth and protein production in mixed cultures.

## RESULTS AND DISCUSSION

### A Fluorescent Reporter of 2′-Fucosyllactose

We hypothesized that since all HMOs contain lactose, specific enzymatic cleavage of modifying sugars would generate lactose, activating the *lac* operon and leading to expression of a reporter protein (in this case, GFP) in proportion to the quantity of the HMO of interest (Figure 1B).

2′-Fucosyllactose (Fuc-α-1,2-Gal-β-1,4-Glc, 2′-FL) is the most abundant oligosaccharide in human milk. As proof of concept, we sought to design a biosensor specific to 2′-FL to be used in conjunction with the biotechnological production of the oligosaccharide.

To defucosylate 2′-FL, we chose the 1,2-α-L-fucosidase domain of the AfcA protein from *Bifidobacterium bifidum*, which is known to be highly specific for α-1,2 fucose linkages (Katayama et al., 2004) and is implicated in the ability of *B. bifidum* to grow on 2′-FL (Ashida et al., 2009). The gene was codon-optimized for *E. coli* (synthesized by Gen9, Cambridge, MA) and synthesized in a cassette downstream of the constitutive J23110 promoter. Because we were not certain that the trisaccharides of interest would be transported across the inner membrane, we directed the glycosidase to the *E. coli* periplasm via N-terminal fusion of the *pelB* signal sequence (ssPelB). This plasmid was named pAfcA. On a second plasmid, we provided GFP under control of the T7 promoter (pET28:GFP).

The plasmids were co-transformed into *E. coli* BL21 (DE3), which contains the T7 RNA polymerase under control of the *lac*UV5 promoter (the strain containing both plasmids is referred to as pAfcA/GFP). When lactose (Galβ1,4Glc) enters the system it induces the *lac* operon, allowing transcription of T7 RNAP. We hypothesized that by monitoring the expression of GFP we could detect the level of 2′-FL that had been defucosylated by the AfcA fucosidase domain (Figure 1B).

To determine the effect of 2′-FL addition on GFP expression, we grew cells containing pAfcA or an empty vector control to mid-log phase and incubated them overnight (16 hr) with either

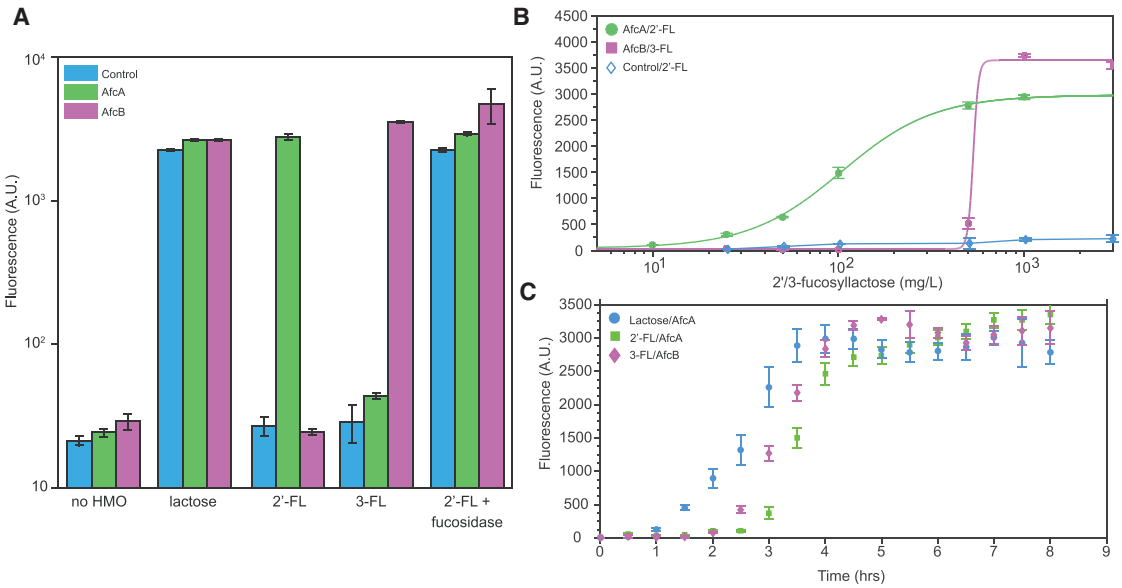


**Figure 2. Characterization of Biosensor for 2′-FL and 3-FL Detection**

(A) Fluorescent detection of 2′-FL and 3-FL. Cells containing pET28:GFP and either pAfcA (green), pAfcB (magenta), or an empty vector control (blue) were induced for 16 hr with no sugar, 2′-FL, 2′-FL with exogenously added α-1,2-fucosidase, 3-FL, or lactose.

(B) Limits of detection and transfer functions of biosensors after 16 hr of incubation. Response curves depicting mean fluorescence (measured in triplicate by flow cytometry) for pAfcA/2′FL (green circle) and pAfcB/3-FL (magenta square) or empty control vector (blue diamond) at varying amounts of trisaccharide cultured as in (A). The dose-response curve was fitted with a 4PL model, shown by the lines.

(C) Time course of reporter expression. Strains pAfcA or pAfcB were incubated with 2′-FL (green square) or 3-FL (magenta diamond), respectively, and fluorescence was monitored over 8 hr of induction. Strain pAfcA incubated with lactose is included as a control. Error bars represent standard deviation of triplicate measurements of mean fluorescence.

no inducer, lactose, 2′-FL, 3-FL (3-fucosyllactose [Gal-β-1,4-(Fuc-α-1,3)-Glc], a trisaccharide isomer of 2′-FL with a different glycosidic linkage). Oligosaccharides were added as molar equivalents to 0.2% (w/v) lactose. All cultures were then analyzed for GFP fluorescence by flow cytometry. Figure 2A shows the mean fluorescence from each induction condition. As expected, lactose induction led to high fluorescence with and without expression of AfcA. In contrast, cells harboring the pAfcA plasmid induced with only 2′-FL had over 100-fold higher fluorescence than cells not expressing pAfcA. In addition, no significant increase in fluorescence was noted when cells were induced with the trisaccharide isomer 3-FL, indicating that the α-1,2 linkage was favored for defucosylation over the α-1,3 linkage. To determine whether this difference was due to the defucosylation of 2′-FL, we induced cells with 2′-FL in media containing exogenous commercial α-1,2-fucosidase (Megazyme), which also led to activation of the *lac* operon (Figure 2A).

## A Fluorescent Reporter of 3-Fucosyllactose

In a similar way, we reasoned that expression of an α-1,3-fucosidase would allow for cleavage and detection of 3-FL. A search of fucosidases in *Bifidobacterium longum* subsp. *infantis* ATCC 15697 (*B. infantis*) revealed the glycosidase *Blon_0426* (which we hereafter refer to as AfcB), which hydrolyzes α-1,3-linked L-fucose (Sela et al., 2012). We amplified the fucosidase domain of the *Blon_0426* gene from the genomic DNA of *B. infantis* and replaced the *afcA* gene in the pAfcA plasmid, creating pAfcB. pAfcB and pET28:GFP were co-transformed into BL21 (DE3) cells as above. Cultures were induced as above and incubated for 16 hr. In the case of induction with 0.3% 3-FL, we observed a roughly 150-fold higher mean fluorescence than that in cells expressing pAfcA or no glycosidase (Figure 2A). Importantly, no change in fluorescence was noted on induction with 0.3% 2′-FL. Thus cells expressing the α-1,2-fucosidase AfcA were responsive to 2′-FL and not 3-FL and cells expressing α-1,3-fucosidase AfcB were responsive to 3-FL and not 2′-FL, demonstrating the linkage specificity of the sensor and the ability to distinguish between isomeric trisaccharides.

## Limits of Detection of Fucosylated Trisaccharides

To evaluate the sensitivity of this assay, we characterized the fluorescent response to varying levels of 2′-FL and 3-FL to estimate the dynamic range and limits of detection. For pAfcA and 2′-FL, the dynamic linear range of detection was found to be between 40 and 400 mg/L and the limit of detection at 4 mg/L (Figure 2B). To put this level in context, *E. coli* strains have been engineered to synthesize 2′-FL at concentrations up to 21.1 g/L (Baumgärtner et al., 2013) and the concentration of 2′-FL in human milk of secretor mothers ranges from 649 to 3,880 mg/L (Goehring et al., 2014), which upon dilution prior to analysis can be measured well within the linear range. The experimental data were fitted into a 4-parameter logistic model (4PL) using MATLAB (Figure 2B). The resulting transfer functions revealed the dynamic range and the minimum/maximum expression levels (Table S1). For pAfcB and 3-FL, the dynamic range of detection was more narrow, between 400 and 600 mg/L, and the limit of detection 350 mg/L. Interestingly, 2′-FL with AfcA had a lower detection limit and more extended dynamic range than

3-FL with AfcB. We speculated that this difference may be due to differences in the activities of these enzymes. Quantification of the enzyme activities revealed the intracellular enzyme concentration to be at 0.6 U/L for the AfcA and 3.5 U/L for AfcB. Given the respective $k_{cat}$ values of these enzymes: 160 $s^{-1}$ for AfcA and 4.48 $s^{-1}$ for AfcB (Sela et al., 2012), we estimated periplasmic protein concentrations as 62.5 pM for AfcA and 13 nM for AfcB. Thus, we attribute the difference in transfer functions to the roughly 200-fold higher expression of AfcB. We note that the constitutive promoter J23110 is quite strong and that substitution for a weaker promoter may improve the dynamic range of the 3-FL assay.

While in initial experiments we induced with trisaccharide overnight (ca. 16 hr), we sought to determine the induction time required to obtain a usable fluorescent signal. To quantify this more precisely, we used flow cytometry at specific time points to generate snapshot measurements of the dynamics of reporter expression (Figure S1). Figure 2C shows fluorescent output from cells containing plasmids pAfcA/pAfcB and pET28:GFP at various time points after induction with either lactose, 2′-FL, or 3-FL. The signal was found to saturate after approximately 5 hr, meaning that this technique can be used within the span of a normal workday. There is a notable lag phase for pAfcA/GFP cultures incubated with 2′-FL, which we attribute to the time taken to defucosylate 2′-FL and transport lactose into the cell for induction of the reporter protein. The lag phase is considerably shorter for pAfcB/GFP cultures grown in 3-FL.

## Detection of 2′-FL from Cell Lysate of a Producer Strain

Having established that the biosensor can specifically and sensitively detect 2′-FL, we next sought to adapt this platform for use in a biotechnological context. Recently, Baumgärtner et al. (2013) developed a strain capable of producing 2′-FL at levels of up to 21 g/L using lactose as a substrate. We cultured this producer strain (JM109 gwBC-F2) and quantified 2′-FL production using LC-MS from a standard curve made by adding defined amounts of 2′-FL to lysate from a non-producer strain (JM109-gwBC) grown under identical conditions (Figures S2A–S2C). We added cell lysate from the producer strain to cultures containing the pAfcA/GFP cells and assayed the GFP expression from these cultures. Figure 3E shows the fluorescent readout for 2′-FL containing cell lysate versus the established standard curve, along with the 4PL model. The models are in good agreement, as seen from the Hill coefficients under the two conditions (Table S1). Higher variability between the signals was observed as more lysate was added to the system, which we attribute to inhibition of either glycosidase activity or GFP expression by unknown components of cell lysate.

## Reducing Signal from Lactose as False Positive

The presence of lactose in milk or in biotechnological processes could lead to false positives, so it is desirable for the sensor to be selective for HMOs over lactose. To remove the residual lactose the cultures may be pelleted and washed, as seen in the control in Figure 3E. However, as this step can be time consuming, we hypothesized that for applications containing lactose, the lactose could instead be selectively enzymatically degraded. To this end, we incubated pAfcA/GFP cells with 0.2% lactose or 0.3% 2′-FL in the presence of varying amounts of exogenous commercial β-galactosidase (Figure 3B). For cells induced with lactose for 16 hr, the fluorescence signal was 20% of the original signal, while with 2′-FL the signal was at 80% when treated with 12 units of β-galactosidase.

Although this strategy effectively reduces signal from lactose, the requirement for purified enzyme is somewhat restrictive. With the same strategy in mind, we hypothesized that wild-type BL21 (DE3) cells added in a preincubation step would metabolize residual lactose, leaving behind the 2′-FL, which these cells cannot use as a carbon source. In addition, these cells would also be incapable of proliferating in the downstream assay which uses antibiotics for plasmid selection. When incubated with lactose (0.2%) for 3 hr, the signal dropped to its background level whereas the signal stayed the same when incubated with 0.3% 2′-FL (Figure 3C). Interestingly, when spiked with equimolar lactose and 2′-FL (0.1% and 0.15%, respectively), the signal dropped to levels comparable with what was observed with the same concentration of 2′-FL.

Finally, we hypothesized that addition of ethanol would simultaneously selectively precipitate lactose (Matsuki et al., 2016) and lyse cells. We incubated the producer strain and the control in two volumes of ethanol for 4 hr and the lysate obtained was kept at 4°C overnight for the lactose to precipitate. Upon filtration, they were tested at different concentrations with the biosensing cells (Figure 3D). A 2-fold drop in fluorescence was observed compared with cells not treated with ethanol and roughly 3-fold higher signal compared with the non 2′-FL-producing control cells. Despite being a simple extraction process, the recovery of the 2′-FL is lower compared with other methods, possibly from losses due to some crystallization of 2′-FL. No significant inhibition of growth of the biosensor cells was observed, owing to the low final ethanol concentrations (<2%) in the cultures. Optimization of this protocol could minimize losses and greatly simplify the assay by eliminating the need for a lysis step. Having demonstrated that the biosensor can be used to detect 2′-FL in strains engineered for production, these strategies of lactose removal can greatly improve the throughput and selectivity of the biosensor. In summary, we have demonstrated several techniques for the selective removal of lactose from the assayed sample. First, washing cells before lysis reduces background significantly (Figure 3E). Next, lactose can be degraded selectively by incubation with either commercial β-galactosidase (Figure 3B) or cells capable of consuming lactose (e.g., BL21) (Figure 3C). While these strategies effectively remove most background lactose, they require an incubation period. Finally, ethanol can be added to the culture to selectively precipitate lactose, which is also effective but reduces overall signal and requires filtration or decanting (Figure 3D). The optimal lactose removal strategy will vary by user priorities including cost, time, throughput, and equipment availability. Overall, for most applications removal using BL21 cells is inexpensive and high-throughput as it can be performed on many cultures in parallel; however, it adds 3 hr to the detection process. Figure 3A summarizes a general workflow for detection of 2′-FL in a producer strain with strategies to fill the gap for reducing false positives.

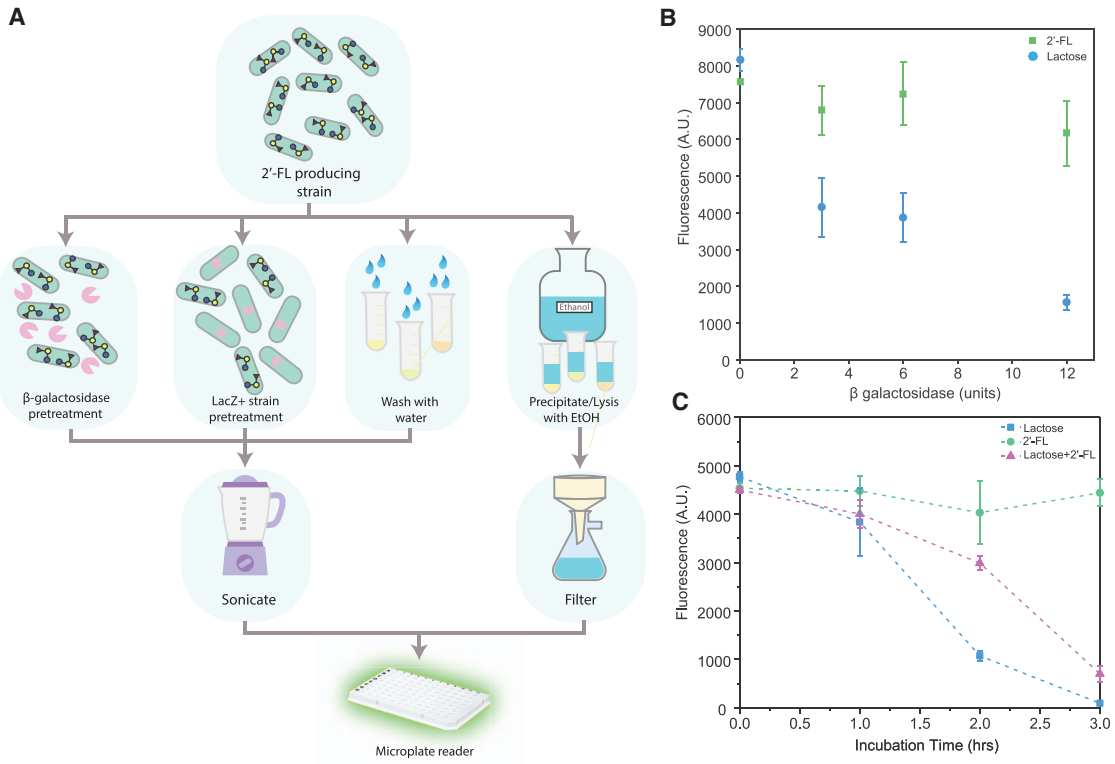


**Figure 3. Biosensor Use in the Context of Biotechnology**

(A) Workflow demonstrating the use of the biosensor in a simple protocol.

(B) Lactose removal by enzymatic digestion. Cultures containing 0.3% 2′-FL (green square) or 0.2% lactose (blue circle) were incubated with biosensor cultures containing varying amounts of exogenous β-galactosidase at induction time were assayed for fluorescence after 16 hr of incubation.

(C) Lactose removal by incubation with wild-type cells. LB containing 0.3% 2′-FL (green circle), 0.2% lactose (blue square), or a 50:50 mixture (0.2% lactose equivalent, magenta triangle) was incubated for various times with BL21 (DE3) cells then added to biosensor cultures for fluorescence measurement after 16 hr of incubation.

(D) Lactose removal and cell lysis by ethanol pretreatment. Fermentations of JM109 gwBC-F2 (magenta circle) or JM109 gwBC (blue triangle) cells were incubated with 2 volumes of ethanol and filtered before incubation with fluorescent biosensor cells and compared with fluorescence from untreated JM109 gwBC-F2 culture (green square).

(E) Quantification of 2′-FL in cell lysate. The biosensor was evaluated for its ability to detect 2′-FL from a metabolically engineered producer strain. Fluorescence measurements generated by addition of either crude lysate of JM109 gwBC-F2 (magenta circle, 2′-FL as quantified by LC-MS), 2′-FL in defined amounts to non-producer strain JM109 gwBC cell lysate (green square), or crude lysate of JM109 gwBC strain (blue diamond).

All fluorescence values represent mean fluorescence from flow-cytometry experiments averaged between three biological replicates. Vertical error bars represent standard deviations of mean fluorescence from triplicate measurements and horizontal error bars represent the variation in 2′-FL measured by high-performance liquid chromatography in the three replicates.

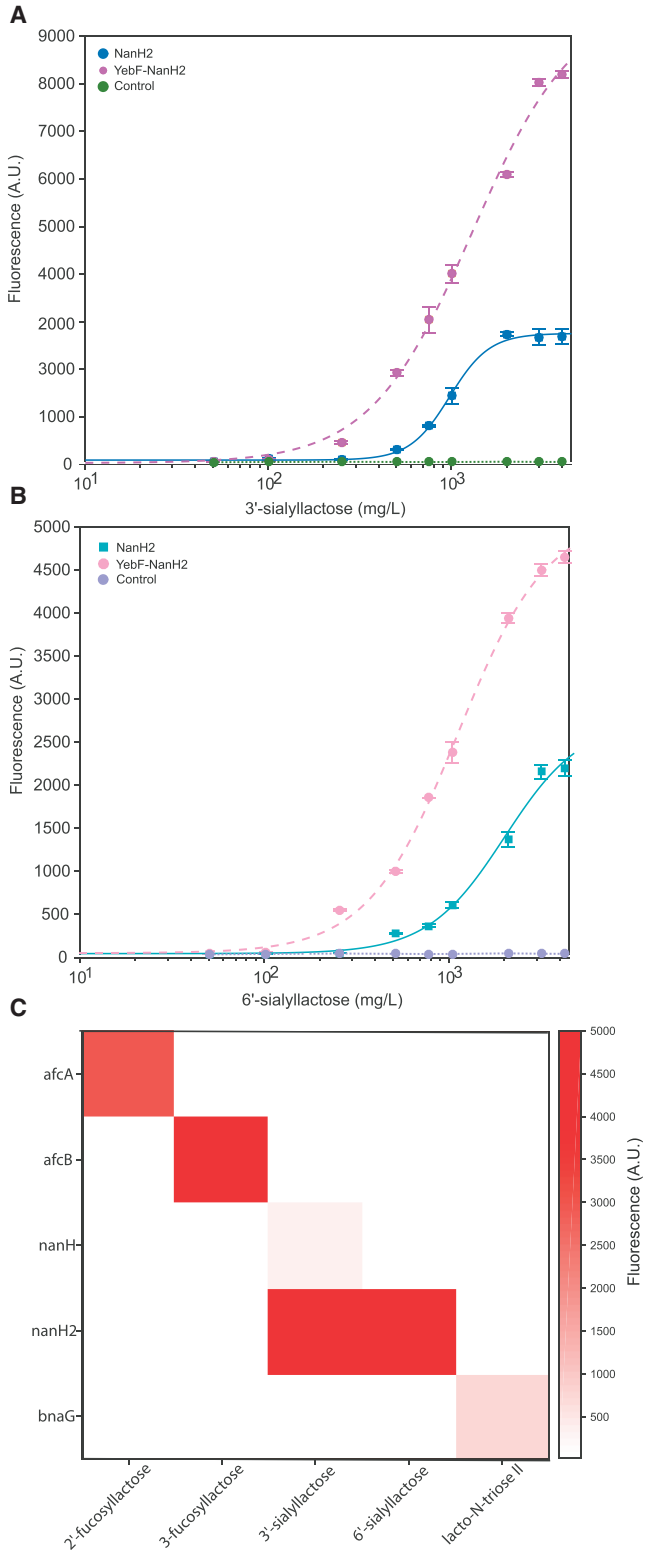


**Figure 4. Substrate Specificity of Glycosidases**

(A) Dose-response curve of biosensor for detection of 3′-SL. Two variants pNanH2 (blue) and pYebF-NanH2 (magenta) were induced with 3′-SL. Cells lacking the plasmid (green) were used as a control.

(B) Dose-response curve of biosensor for detection of 6′-SL. Similarly, two variants pNanH2 (teal), pYebF-NanH2 (pink), and the control (lavender) were induced with 6′-SL as in (A).

(C) Heatmap showing the range of biosensors created and tested for orthogonality. Heatmap represents mean fluorescence of cell cultures expressing the indicated glycosidase induced with equivalent of 0.2% lactose of indicated sugars. All cultures were induced overnight. All error bars represent standard deviations of triplicate measurements of mean fluorescence.

## Detection of Sialylated and *N*-Acetylglucosaminylated Trisaccharides

The demonstrated ability to differentiate between fucosylated isomers of different linkages inspired us to expand the capability of our biosensor to other modifications of lactose present in HMOs. To accomplish this, we synthesized and codon-optimized or amplified from genomic DNA three more genes, as with *afcA*, and incorporated them into our secretion and expression plasmid. The glycosidases chosen were: (1) *nanH2* from *B. infantis*, a sialidase known to hydrolyze both α-2,3 and α-2,6 sialic acid linkages (Sela et al., 2011); (2) *nanH* from *Pasteurella multocida*, an α-2,3 sialidase with activity on 3′-SL (Mizan et al., 2000); and (3) the lacto-*N*-biosidase domain (corresponding to residues 32–533) of the *bnaG* gene from *Lactobacillus casei*, previously demonstrated to be essential for hydrolysis of lacto-*N*-triose II (GlcNAc-β-1,3-Gal-β-1,4-Glc, LNT II) in this organism and other related lactobacilli (Bidart et al., 2016).

First, we measured the fluorescent response of the biosensor to 3′-SL using *B. infantis* NanH2 as the glycosidase. When incubated with 0.4% 6′-SL, we observed an over 100-fold increase in mean fluorescence compared with cells not expressing the sialidase. The mean fluorescence also increased in response to the addition of 3′-SL, in accordance with previously observed broader substrate specificity of this enzyme (Sela et al., 2011) (Figure 4A), but the overall response to sialylated HMOs was not as robust as that of the fucosylated HMOs. We hypothesized that this was a result of negatively charged sialyllactose facing electrostatic mass transfer resistance across the *E. coli* outer membrane. To overcome this barrier, we created an N-terminal fusion of NanH2 to the *E. coli* YebF protein, which has been shown to direct extracellular protein secretion in *E. coli* (Haitjema et al., 2014; Zhang et al., 2006). We used a commercially available neuraminidase assay kit (Millipore Sigma) to determine the sialidase activity in the extracellular media when fused with the YebF protein. Only trace levels of sialidase activity were observed for the periplasmic NanH2 construct compared with the YebF-NanH2 fusion where the majority accumulated in the extracellular medium (Figure S3A). When NanH2 was fused with YebF and secreted extracellularly, the fluorescent response was roughly 3-fold higher and comparable with that of fucosylated HMOs with their respective fucosidases (Figure 4A).

As NanH2 has been shown to have activity on both 3′-SL and 6′-SL, we noted a similar qualitative trend in the fluorescent response of NanH2-producing cells to 6′-SL (Figure 4B). In cells expressing the YebF-NanH2 fusion protein, the fluorescent response was again higher than with periplasmically expressed NanH2. However, while the limits of detection for 3′-SL and 6′-SL were similar, the overall fluorescent response to 0.4% 6′-SL was lower compared with 0.4% 3′-SL. Kinetic data observed by Sela et al. (2011) showed a 2-fold lower catalytic

efficiency (attributable to a 2-fold higher $K_M$ with comparable $k_{cat}$ values) for a 3′-sialylated substrate ($K_M$: 7.8 mM) than its 6′-sialylated counterpart ($K_M$: 3.8 mM). This difference would suggest an approximately 1.4-fold higher activity on 6′-SL at the amounts assayed (approximately 6.3 mM in the media). While the reason for this slight discrepancy is not clear, we demonstrate that sialic acid-containing HMOs can be detected reliably in our system.

To test whether a highly specific sialidase could be used to detect a specific sialic acid linkage, we expressed *P. multocida* NanH, which has a 50-fold higher activity on an α-2,3 linked (4-methylumbelliferyl-3′-SL) compared to a 6′-sialylated substrate (4-MU-6′-SL) (Mizan et al., 2000), in both the periplasmic (ssPelB fusion) and extracellular (YebF fusion) spaces. In the case of periplasmic expression, we saw very low fluorescence even at 0.4% 3′-SL. However, the YebF fusion to this protein contributed a measurable signal. Comparison of sialidase activity of the supernatant for YebF-NanH and YebF-NanH2 variants using 3′-SL as a substrate revealed a roughly 900-fold lower activity for NanH compared with NanH2 (0.036 U/L in supernatant of YebF-NanH versus 32 U/L in supernatant of YebF-NanH2). Using available kinetic parameters on 4-MU-3′-SL for both enzymes as a proxy for activity, we estimate that the difference in activity corresponds to roughly 380-fold lower (2.2 pM versus 840 pM) enzyme expression, suggesting that functional expression and/or translocation of *P. multocida* NanH is limited in this system and is a target for further optimization of expression. Even so, we were still able to observe fluorescence well above background for 3′-SL in the NanH case, while no fluorescent signal was observable when NanH cells were incubated with 6′-SL (Figure 4C).

Finally, we tested the *N*-acetylgalactosaminidase domain of BnaG from *L. casei*, known to hydrolyze LNT II. Cells expressing this glycosidase had a moderate fluorescent response at 0.3% LNT II (Figure 4C). BnaG, although specific to GlcNAc-β-1,3-glycosidic linkages, only possesses exoglycosidase activity (Bidart et al., 2016). This was demonstrated by the lack of signal when tested with lacto-*N*-neotetraose, which contains the same but non-terminal β-1,3-linked GlcNAc (Figure S3B).

Taken together, we demonstrated the action of five different glycosidase enzymes on five different HMO substrates. As a final proof of the orthogonality of detection in our system, we tested each of the five substrates individually with cells expressing each of the five enzymes (Figure 4C). Very little mean fluorescence was detected for the non-target oligosaccharides (off diagonal), except for the case of NanH2, which is known to hydrolyze both 6′-SL and 3′-SL and behaved accordingly. Thus, we conclude that our assay facilitates quantitative fluorescent detection of five different HMOs in a manner specific to the glycosidic linkage associated with the chosen enzyme.

## HMOs Can Be Used as a Sole Carbon Source in Engineered Strains

Previous studies have reported that bifidobacteria thrive by consuming oligosaccharides in the infant gut (Marcobal et al., 2010; Ward et al., 2007). This prompted us to assess the ability of our engineered *E. coli* to utilize HMOs as a carbon source. *E. coli* BL21 (DE3) containing pAfcA were cultured in M9 minimal media containing 0.2% lactose, 0.3% 2′-FL, or 0.3% 3-FL as a sole carbon source. The strain demonstrated growth on both carbohydrate substrates (Figure 5A). During growth on lactose, there was a lag phase of approximately 1 hr followed by normal exponential growth with a specific growth rate of 0.09 $hr^{-1}$. Interestingly, the length of lag phase increases when using 2′-FL as the carbon source compared with lactose, which we suggest represents the time component of hydrolysis of 2′-FL into lactose in the LacZ + strain BL21 (DE3). The specific growth rate, however, remains comparable with that observed in lactose and also the specific growth rate in glucose, 0.1 $hr^{-1}$. We also cultured biosensing cells harboring the pAfcB plasmid with 2′/3-FL. These cells demonstrated a similar specific growth rate but a considerably shorter lag phase (15 hr) compared with pAfcA. No growth was observed for cells in the absence of a carbon source or for cells expressing AfcB in media containing 2′-FL.

## Prebiotic Enrichment of Strains in Mixed Culture

The ability to hydrolyze complex carbohydrates is a key determining factor in the proliferation of individual strains in complex microbial environments (Flint et al., 2008). Competition among the strains results in the dominance of the population expressing the carbohydrate hydrolyzing phenotype. Since we had established growth on HMOs in *E. coli*, we tested whether we could control the relative abundance of a particular strain in a mixed culture by varying the carbohydrate source. To examine the dynamics of HMO-utilizing *E. coli* strains in a mixed culture environment, we co-cultured two BL21 (DE3) strains harboring either pAfcA or pAfcB in minimal media with HMOs as a sole carbon source and evaluated their relative abundance. Mixtures with relative abundances varying from 1:1 to 1:100 of pAfcA and pAfcB cells were inoculated into M9 media containing either 2′-FL, 3-FL, or lactose. After culturing for 36 hr, approximately 500 CFU were plated on non-selective media and grown overnight at 37°C. From these plates, approximately 50 colonies were used as templates for colony PCR amplification with primers specific for either the *afcA* or *afcB* genes. The results of these colony PCR characterizations are shown in Figure 5B and Table S2. As expected, when cells were grown on lactose with a 1:1 inoculum ratio, the ratio of AfcA:AfcB colonies was approximately 1:1 (14/26 AfcA). However, in the presence of 2′-FL, cells expressing pAfcA were much more abundant (>90%) than the original inoculum ratios, demonstrating enrichment at a level far greater than chance ($p < 0.0001$). Similarly, in the presence of 3-FL, pAfcB cells were greatly enriched as well (>95%). This result demonstrates growth-based selection for glycosidase activity or HMO utilization in mixed culture providing a selection-based option for directed evolution studies in addition to the already established fluorescent screen.

A mixed population of biosensors designed to respond to different inputs must be able to distinguish between them. To monitor for crosstalk between microbial strains (e.g., growth of a strain not engineered to use the substrate of interest), we transformed cells expressing AfcA with pET28:GFP and cells expressing AfcB with a pET28 vector containing the red fluorescent protein mCherry. We expected that during growth on minimal media, only cells able to use a particular HMO as a carbon source would grow and that fluorescent protein expression would be induced in those cells, allowing red or green fluorescence to serve as a proxy for real-time analysis of population

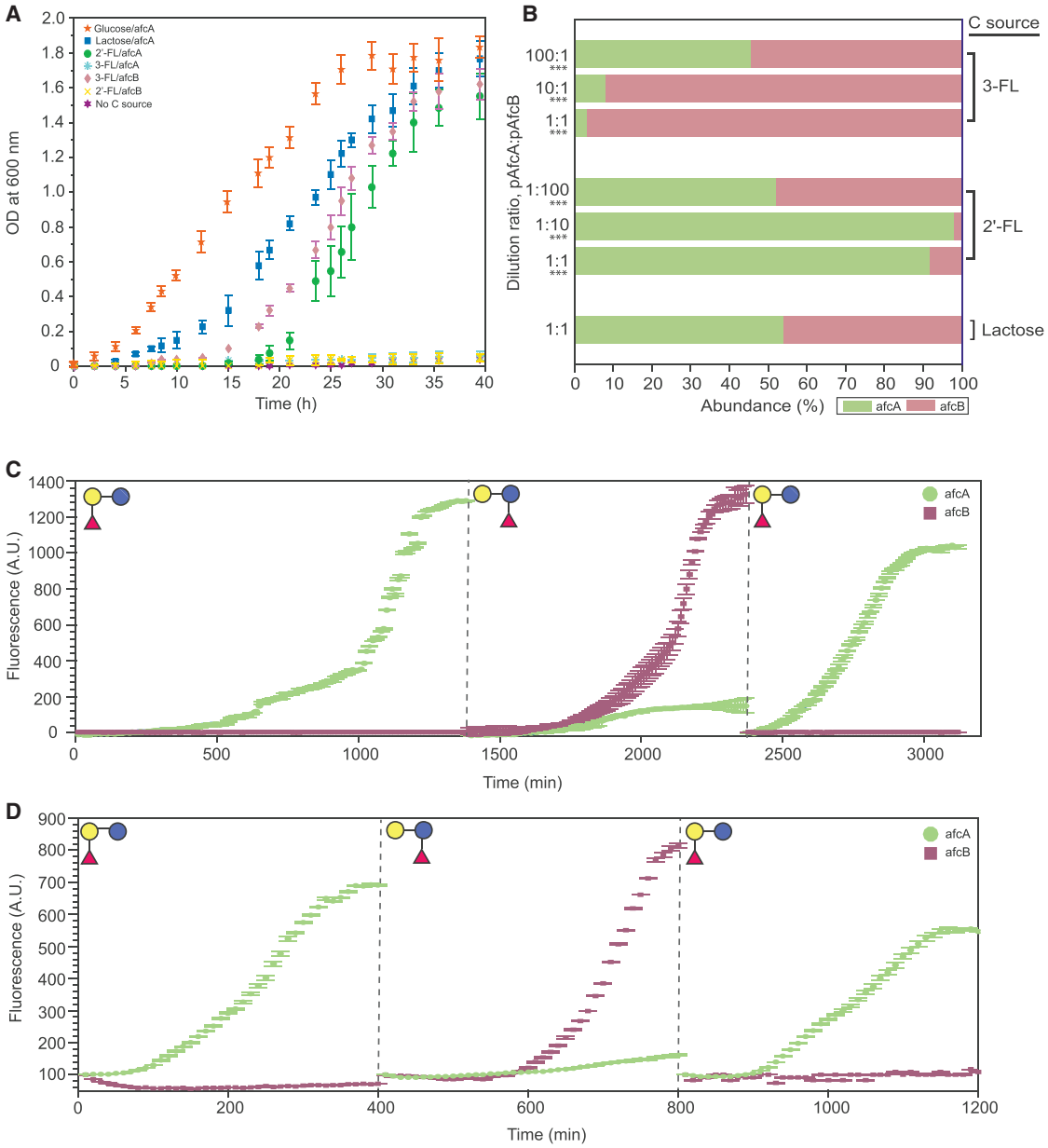


**Figure 5. Prebiotic Enrichment and Dynamic Control of Mixed Culture**

(A) Growth kinetics of pAfcA on glucose (orange pentagram), lactose (blue square), 2′-FL (green circle), 3-FL (turquoise asterisk), and no carbon source (purple star) and of pAfcB on 3-FL (magenta diamond) or 2′-FL (yellow cross).

(B) Population distribution after growth in lactose, 2′-FL, or 3-FL. Measurements were made by plating the enriched cultures on non-selective media and performing colony PCR for *afcA* or *afcB* genes. Colonies were selected from three independent plates (technical replicates) from two biological replicates. For statistical analysis, we modeled the population using a binomial distribution to conclude for each dilution ratio that the enrichment of the strain was not due to chance but dependent on the carbon source. The triple asterisk (***) represents a probability of <0.0001 that the result followed a binomial distribution with respect to the observed lactose control.

(C) GFP and mCherry fluorescence readings from the enrichment procedure with three rounds of enrichment. 1:1 mixtures of pAfcA/GFP (green circle) and pAfcB/mCherry (magenta square) biosensors were grown minimal media with the indicated substrates. After the end of log phase, cultures were diluted 100:1 and incubated in fresh minimal media containing the HMO of interest as the carbon source.

(D) GFP and mCherry fluorescence measurements of pAfcA/GFP (green circle) and pAfcB/mCherry (magenta square) biosensors co-cultured in rich media with the HMO of interest as inducer. All error bars represents standard deviation of triplicate measurements of mean fluorescence.

dynamics. Cells expressing AfcA/GFP and AfcB/mCherry were mixed at a 1:1 ratio and cultured in M9 with 0.3% 2′-FL. In agreement with the colony PCR results from Figure 5B, cells with green fluorescence dominated the population during culture and virtually no red fluorescence was detected. On the other hand, the same population cultured in lactose displayed roughly equal

**Table 1. Strains and Plasmids Used in This Study**

| Strain/Plasmid | Genotype and/or Description | Source/Reference |
|---|---|---|
| *E. coli* BL21 (DE3) | fhuA2 [lon] ompT gal (λ DE3) [dcm] ΔhsdS<br>λ DE3 = λ sBamHIo ΔEcoRI-B int::(lacI::PlacUV5::T7 gene1) i21 Δnin5 | New England Biolabs |
| *E. coli* NEB 5-alpha | fhuA2 Δ(argF-lacZ)U169 phoA glnV44 Φ80 Δ(lacZ)M15 gyrA96 recA1 relA1 endA1 thi-1 hsdR17 | New England Biolabs |
| pET28:GFP | $Kan^R$, pT7/LacO:GFP | Shis and Bennett, 2013 |
| pET28:mCherry | $Kan^R$, pT7/LacO:mCherry | this study |
| pAfcA | $Amp^R$, pG9-m2 vector with *B. bifidum afcA* under pJ23110 with N-terminal PelB signal sequence | this study |
| pAfcB | pAfcA with *afcA* replaced by *B. infantis afcB* | this study |
| pNanH | AmpR, pG9-m2 vector with *P. multocida nanH* under pJ23110 with N-terminal PelB signal sequence | this study |
| pNanH2 | pAfcA with *afcA* replaced with *B. infantis nanH2* | this study |
| pYebF-NanH | pNanH with N-terminal fusion of *E. coli* YebF replacing N-terminal signal sequence | this study |
| pYebF-NanH2 | pNanH2 with N-terminal fusion of *E. coli* YebF replacing N-terminal signal sequence | this study |
| pBnaG | $Amp^R$, pG9-m2 vector with *L. paracasei bnaG* under control of constitutive promoter with N-terminal PelB signal sequence | this study |

fluorescence throughout the course of growth (Figure S4A). When this culture reached the end of exponential phase, the cells were washed and diluted at a ratio of 1:100 into M9 media with 3-FL. This time a red fluorescent population dominated, indicative of the abundance of the AfcB-producing strain. Notably, near the end of the exponential phase a relatively small amount of green fluorescence began to appear. We believe that this is indicative of extracellular hydrolysis of 3-FL by AfcB via leakage or some other mechanism (Georgiou et al., 1988; Hancock, 1984) and is a small source of crosstalk. However, we note that the red fluorescent signal is still significantly higher (roughly 9-fold) and only appears after a few hours of growth. Finally, after reaching the end of exponential phase, the population was washed again and diluted 1:100 in M9 with 2′-FL. Green fluorescence again dominated the population with very little red fluorescent background. We repeated the enrichment cycle in 2′-FL to determine whether a similar high red fluorescence signal was observed. It is unclear why some crosstalk seems to occur in the 3-FL cultures but not 2′-FL cultures. However, leakage of enzymes from the periplasmic space is common, especially in the case of heterologous expression (Georgiou et al., 1988), and is often inversely proportional to protein size (Rinas and Hoffmann, 2004). The expressed AfcB protein is approximately half the molecular weight of the AfcA protein (50.36 kDa versus 96.76 kDa), making it more likely to leak into the extracellular milieu and hydrolyze 3-FL to lactose in the media. We also speculate that the 13-fold higher catalytic efficiency of AfcB relative to AfcA (Sela et al., 2012) enables increased hydrolytic activity. We thus demonstrated that the selective pressure exerted by the single carbon source promotes controlled colonization, which mirrors natural strategies exhibited by probiotic bacteria.

## Dynamic Control of Protein Expression in Mixed Culture with HMOs

Recently, engineered microbial consortia have been used to divide tasks between constituent strains or to change enzymatic expression as substrates are depleted (Brenner et al., 2008; Jones et al., 2017; Zhou et al., 2015). As proof of principle, we sought to demonstrate our ability to control expression of different proteins in mixed cultures of *E. coli* strains using HMOs as inducers. We hypothesized that only in strains equipped to hydrolyze a particular HMO to lactose would the lac operon be induced, thus providing orthogonal control over protein expression in mixed cultures. To accomplish this, we inoculated 1:1 cultures of the AfcA/GFP and AfcB/mCherry strains mentioned above, this time culturing them in rich media (Luria-Bertani [LB]). Lactose trials indicated that all cells are capable of growth and expression, irrespective of the glycosidase expressed (Figure S4B). These results stimulated additional experiments similar to those detailed in Figure 5B, using rich media to ensure growth of both strains, to determine crosstalk between mixed cultures. When cultured in LB media with 2′-FL, we observed high GFP expression but little mCherry expression (Figure 5D). When cells were washed and diluted into 3-FL, the mCherry signal dominated, and similarly the GFP signal dominated when the media were switched back to 2′-FL. We thus demonstrate orthogonal, dynamic control of protein expression in an unbiased mixed culture via induction using HMOs.

## Conclusions

In this work we developed a rapid, non-chromatographic, whole-cell biosensor for quantification and linkage analysis of five different HMOs, covering three of the major modifications to the lactose core: the addition of fucose, sialic acid, and GlcNAc. Since all HMOs contain a lactose core, we submit that this method can be easily expanded to higher-order human milk oligosaccharides such as lacto-*N*-fucopentaose or 3-fucosyl-3′-sialyllactose by combinatorial expression of glycosidases. The throughput of this technique will allow optimization of both synthetic and biotechnological processes for the manufacture of HMOs, as many reaction conditions or bioreactor parameters could be assayed at once (in multi-well format) in a matter of

hours. We also demonstrate the growth of *E. coli* on HMOs as a single carbon source, providing a growth selection to complement the established fluorescent screening. In addition to optimization of bioprocessing, this technology lays the groundwork for the use of directed evolution to engineer improved linkage-specific glycosidases, enabling the expansion of a burgeoning glycobiology toolbox.

We also established the use of HMOs as a modulator of bacterial population in mixed cultures, selectively favoring the growth of the strain with the ability to metabolize the HMO of interest. This phenomenon closely mirrors the relationship between prebiotic HMOs and bifidobacteria in the infant gut (Sela and Mills, 2010) and serves as a springboard for the use of these prebiotics to manipulate population dynamics and protein expression in engineered microbial communities. Taken together, these applications have broad implications in, e.g., mechanistic studies of the microbiome and the use of microbial consortia in metabolic engineering of complex high-value products (Brenner et al., 2008). Methods such as these will help to expand our knowledge of the synergistic interplay of prebiotics and probiotics in both the natural holobiont and synthetic microbial communities.

## SIGNIFICANCE

**In this work we developed a whole-cell biosensor for the high-throughput detection of human milk oligosaccharides (HMO), which are important prebiotic complex carbohydrate components of human breast milk. With growing interest in biotechnology for HMO synthesis, owing to its beneficial effects on the infant gut microbiota, high-throughput screening is key to optimization of biosynthesis. Current detection technology is limited by its throughput, cost, and complexity, and determination of glycosidic linkage is particularly difficult. We leveraged the unique specificity of glycosidase enzymes to create a synthetic *in vivo* genetic circuit that allows non-chromatographic, high-throughput, glycosidic linkage-specific, sensitive, and orthogonal detection of lactose-based HMOs. We also demonstrated orthogonal, dynamic regulation of growth and protein expression of selected strains in mixed cultures, mimicking the prebiotic effect of these compounds. This biosensor platform has the potential to be used as a basis for directed evolution of enzymes in the biosynthesis pathway and as a tool to modulate the population dynamics of natural and engineered microbial communities. Taken together, these results demonstrate that our whole-cell biosensor can be leveraged toward a broad range of biological applications including, but not limited to, (1) optimization of synthetic, chemoenzymatic, and biotechnological synthesis of HMOs, (2) dynamic manipulation of microbial populations and protein expression in those populations, and (3) increasing the availability of HMO molecules to broaden the scope of research on these important biomolecules.**

## STAR★METHODS

Detailed methods are provided in the online version of this paper and include the following:



## SUPPLEMENTAL INFORMATION

Supplemental Information includes four figures, three tables, and one data file and can be found with this article online at https://doi.org/10.1016/j.chembiol.2018.06.002.

## ACKNOWLEDGMENTS

This work was supported by Iowa State University Startup Funds. T.J.M. was partially supported by the Karen and Denny Vaughn Faculty Fellowship. Strains JM109 gwBC and gwBC-F2 were a generous gift of Dr. Georg Sprenger (Universität Stuttgart). Plasmid pET28:GFP was a gift from Matthew Bennett (Addgene plasmid #60733). The mCherry gene was amplified from plasmid pHL 1277, a gift from Han Lim (Addgene plasmid #53017). We thank Dr. Shawn M. Rigby of the Iowa State University Flow Cytometry Facility and the W.M. Keck Metabolomics Research Laboratory for assistance with fluorescence and LC-MS studies.

## AUTHOR CONTRIBUTIONS

Conceptualization, T.J.M.; Methodology, T.J.M. and F.E.; Investigation and Validation, F.E.; Writing, T.J.M. and F.E.; Visualization, T.J.M. and F.E.; Supervision, T.J.M.

## DECLARATION OF INTERESTS

The authors declare no competing interests.

Received: November 26, 2017
Revised: March 10, 2018
Accepted: June 1, 2018
Published: July 12, 2018

## REFERENCES

Abatemarco, J., Hill, A., and Alper, H.S. (2013). Expanding the metabolic engineering toolbox with directed evolution. Biotechnol. J. *8*, 1397–1410.

Alderete, T.L., Autran, C., Brekke, B.E., Knight, R., Bode, L., Goran, M.I., and Fields, D.A. (2015). Associations between human milk oligosaccharides and infant body composition in the first 6 mo of life. Am. J. Clin. Nutr. *102*, 1381–1388.

Angeloni, S., Ridet, J.L., Kusy, N., Gao, H., Crevoisier, F., Guinchard, S., Kochhar, S., Sigrist, H., and Sprenger, N. (2005). Glycoprofiling with micro-arrays of glycoconjugates and lectins. Glycobiology *15*, 31–41.

Ashida, H., Miyake, A., Kiyohara, M., Wada, J., Yoshida, E., Kumagai, H., Katayama, T., and Yamamoto, K. (2009). Two distinct alpha-L-fucosidases from *Bifidobacterium bifidum* are essential for the utilization of fucosylated milk oligosaccharides and glycoconjugates. Glycobiology *19*, 1010–1017.

Baumgärtner, F., Seitz, L., Sprenger, G.A., and Albermann, C. (2013). Construction of *Escherichia coli* strains with chromosomally integrated expression cassettes for the synthesis of 2'-fucosyllactose. Microb. Cell Fact. *12*, 1–13.

Baumgärtner, F., Conrad, J., Sprenger, G.A., and Albermann, C. (2014). Synthesis of the human milk oligosaccharide lacto-N-tetraose in metabolically engineered, plasmid-free *E. coli*. Chembiochem *15*, 1896–1900.

van den Berg, R., Peters, J.A., and van Bekkum, H. (1994). The structure and (local) stability constants of borate esters of mono- and di-saccharides as studied by $^{11}B$ and $^{13}C$ NMR spectroscopy. Carbohydr. Res. *253*, 1–12.

Bidart, G.N., Rodríguez-Díaz, J., and Yebra, M.J. (2016). The extracellular wall-bound β-N-acetylglucosaminidase from *Lactobacillus casei* is involved in the metabolism of the human milk oligosaccharide lacto-N-triose. Appl. Environ. Microbiol. *82*, 570–577.

Brenner, K., You, L., and Arnold, F.H. (2008). Engineering microbial consortia: a new frontier in synthetic biology. Trends Biotechnol. *26*, 483–489.

Chai, W., Piskarev, V.E., Zhang, Y., Lawson, A.M., and Kogelberg, H. (2005). Structural determination of novel lacto-N-decaose and its monofucosylated analogue from human milk by electrospray tandem mass spectrometry and $^{1}H$ NMR spectroscopy. Arch. Biochem. Biophys. *434*, 116–127.

Charbonneau, M.R., Blanton, L.V., DiGiulio, D.B., Relman, D.A., Lebrilla, C.B., Mills, D.A., and Gordon, J.I. (2016). A microbial perspective of human developmental biology. Nature *535*, 48–55.

Chaturvedi, P., Warren, C.D., Altaye, M., Morrow, A.L., Ruiz-Palacios, G., Pickering, L.K., and Newburg, D.S. (2001). Fucosylated human milk oligosaccharides vary between individuals and over the course of lactation. Glycobiology *11*, 365–372.

Chen, R. (2015). The sweet branch of metabolic engineering: cherry-picking the low-hanging sugary fruits. Microb. Cell Fact. *14*, 197.

Chen, L., Valentine, J.L., Huang, C.-J., Endicott, C.E., Moeller, T.D., Rasmussen, J.A., Fletcher, J.R., Boll, J.M., Rosenthal, J.A., Dobruchowska, J., et al. (2016). Outer membrane vesicles displaying engineered glycotopes elicit protective antibodies. Proc. Natl. Acad. Sci. USA *113*, E3609–E3618.

Coppa, G.V., Pierani, P., Zampini, L., Carloni, I., Carlucci, A., and Gabrielli, O. (1999). Oligosaccharides in human milk during different phases of lactation. Acta Paediatr. Suppl. *88*, 89–94.

Crane, J.K., Azar, S.S., Stam, A., and Newburg, D.S. (1994). Oligosaccharides from human milk block binding and activity of the *Escherichia coli* heat-stable enterotoxin (STa) in T84 intestinal cells. J. Nutr. *124*, 2358–2364.

Daunert, S., Barrett, G., Feliciano, J.S., Shetty, R.S., Shrestha, S., and Smith-Spencer, W. (2000). Genetically engineered whole-cell sensing systems: coupling biological recognition with reporter genes. Chem. Rev. *100*, 2705–2738.

Doherty, M., Bones, J., McLoughlin, N., Telford, J.E., Harmon, B., DeFelippis, M.R., and Rudd, P.M. (2013). An automated robotic platform for rapid profiling oligosaccharide analysis of monoclonal antibodies directly from cell culture. Anal. Biochem. *442*, 10–18.

Drouillard, S., Driguez, H., and Samain, E. (2006). Large-scale synthesis of H-Antigen oligosaccharides by expressing *Helicobacter pylori* α1, 2-fucosyltransferase in metabolically engineered *Escherichia coli* cells. Angew. Chem. Int. Ed. *118*, 1810–1812.

Dumon, C., Bosso, C., Utille, J.P., Heyraud, A., and Samain, E. (2006). Production of Lewis x tetrasaccharides by metabolically engineered *Escherichia coli*. Chembiochem *7*, 359–365.

Evangelista, R.A., Liu, M.-S., and Chen, F.-T.A. (1995). Characterization of 9-aminopyrene-1,4,6-trisulfonate derivatized sugars by capillary electrophoresis with laser-induced fluorescence detection. Anal. Chem. *67*, 2239–2245.

La Ferla, B., Prosperi, D., Lay, L., Russo, G., and Panza, L. (2002). Synthesis of building blocks of human milk oligosaccharides. Fucosylated derivatives of the lacto- and neolacto-series. Carbohydr. Res. *337*, 1333–1342.

Flint, H.J., Bayer, E.A., Rincon, M.T., Lamed, R., and White, B.A. (2008). Polysaccharide utilization by gut bacteria: potential for new insights from genomic analysis. Nat. Rev. Microbiol. *6*, 121–131.

Garrido, D., Ruiz-Moyano, S., Kirmiz, N., Davis, J.C., Totten, S.M., Lemay, D.G., Ugalde, J.A., German, J.B., Lebrilla, C.B., and Mills, D.A. (2016). A novel gene cluster allows preferential utilization of fucosylated milk oligosaccharides in *Bifidobacterium longum* subsp. *longum* SC596. Sci. Rep. *6*, 35045.

Georgiou, G., Shuler, M.L., and Wilson, D.B. (1988). Release of periplasmic enzymes and other physiological effects of beta-lactamase overproduction in *Escherichia coli*. Biotechnol. Bioeng. *32*, 741–748.

Goehring, K.C., Kennedy, A.D., Prieto, P.A., and Buck, R.H. (2014). Direct evidence for the presence of human milk oligosaccharides in the circulation of breastfed infants. PLoS One *9*, e101692.

Gonia, S., Tuepker, M., Heisel, T., Autran, C., Bode, L., and Gale, C.A. (2015). Human milk oligosaccharides inhibit *Candida albicans* invasion of human premature intestinal epithelial cells. J. Nutr. *145*, 1992–1998.

Goubet, F., Jackson, P., Deery, M.J., and Dupree, P. (2002). Polysaccharide analysis using carbohydrate gel electrophoresis: a method to study plant cell wall polysaccharides and polysaccharide hydrolases. Anal. Biochem. *300*, 53–68.

Green, A.A., Silver, P.A., Collins, J.J., and Yin, P. (2014). Toehold switches: de-novo-designed regulators of gene expression. Cell *159*, 925–939.

Haitjema, C.H., Boock, J.T., Natarajan, A., Dominguez, M.A., Gardner, J.G., Keating, D.H., Withers, S.T., and DeLisa, M.P. (2014). Universal genetic assay for engineering extracellular protein expression. ACS Synth. Biol. *3*, 74–82.

Hamilton, S.R., Davidson, R.C., Sethuraman, N., Nett, J.H., Jiang, Y., Rios, S., Bobrowicz, P., Stadheim, T.A., Li, H., Choi, B.-K., et al. (2006). Humanization of yeast to produce complex terminally sialylated glycoproteins. Science *313*, 1441–1443.

Han, N.S., Kim, T.-J., Park, Y.-C., Kim, J., and Seo, J.-H. (2012). Biotechnological production of human milk oligosaccharides. Biotechnol. Adv. *30*, 1268–1278.

Hancock, R.E.W. (1984). Alterations in outer membrane permeability. Annu. Rev. Microbiol. *38*, 237–264.

Harms, H., Wells, M.C., and van der Meer, J.R. (2006). Whole-cell living biosensors—are they ready for environmental application? Appl. Microbiol. Biotechnol. *70*, 273–280.

Hung, M., Chang, E., Hussein, R., Frazier, K., Shin, J.-E., Sagawa, S., and Lim, H.N. (2014). Modulating the frequency and bias of stochastic switching to control phenotypic variation. Nat. Commun. *5*, 4574.

Jones, J.A., Vernacchio, V.R., Collins, S.M., Shirke, A.N., Xiu, Y., Englaender, J.A., Cress, B.F., McCutcheon, C.C., Linhardt, R.J., Gross, R.A., et al. (2017). Complete biosynthesis of anthocyanins using *E. coli* polycultures. MBio *8*, https://doi.org/10.1128/mBio.00621-17.

Kailemia, M.J., Ruhaak, L.R., Lebrilla, C.B., and Amster, I.J. (2014). Oligosaccharide analysis by mass spectrometry: a review of recent developments. Anal. Chem. *86*, 196–212.

Katayama, T., Sakuma, A., Kimura, T., Makimura, Y., Hiratake, J., Sakata, K., Yamanoi, T., Kumagai, H., and Yamamoto, K. (2004). Molecular cloning and characterization of *Bifidobacterium bifidum* 1,2-alpha-L-fucosidase (AfcA), a novel inverting glycosidase (glycoside hydrolase family 95). J. Bacteriol. *186*, 4885–4893.

Khalil, A.S., and Collins, J.J. (2010). Synthetic biology: applications come of age. Nat. Rev. Genet. *11*, 367–379.

Kobayashi, H., Kaern, M., Araki, M., Chung, K., Gardner, T.S., Cantor, C.R., and Collins, J.J. (2004). Programmable cells: interfacing natural and engineered gene networks. Proc. Natl. Acad. Sci. USA *101*, 8414–8419.

Kuchner, O., and Arnold, F.H. (1997). Directed evolution of enzyme catalysts. Trends Biotechnol. *15*, 523–530.

Kunz, C., Rudloff, S., Baier, W., Klein, N., and Strobel, S. (2000). Oligosaccharides in human milk: structural, functional, and metabolic aspects. Annu. Rev. Nutr. *20*, 699–722.

Lee, W.-H., Pathanibul, P., Quarterman, J., Jo, J.-H., Han, N.S., Miller, M.J., Jin, Y.-S., and Seo, J.-H. (2012). Whole cell biosynthesis of a functional oligosaccharide, 2′-fucosyllactose, using engineered *Escherichia coli*. Microb. Cell Fact. *11*, 48.

Leveau, J.H.J., and Lindow, S.E. (2002). Bioreporters in microbial ecology. Curr. Opin. Microbiol. *5*, 259–265.

Mally, M., Fontana, C., Leibundgut-Landmann, S., Laacisse, L., Fan, Y.-Y., Widmalm, G., and Aebi, M. (2013). Glycoengineering of host mimicking

type-2 LacNAc polymers and Lewis X antigens on bacterial cell surfaces. Mol. Microbiol. *87*, 112–131.

Marcobal, A., Barboza, M., Froehlich, J.W., Block, D.E., German, J.B., Lebrilla, C.B., and Mills, D.A. (2010). Consumption of human milk oligosaccharides by gut-related microbes. J. Agric. Food Chem. *58*, 5334–5340.

Matsuki, T., Yahagi, K., Mori, H., Matsumoto, H., Hara, T., Tajima, S., Ogawa, E., Kodama, H., Yamamoto, K., Yamada, T., et al. (2016). A key genetic factor for fucosyllactose utilization affects infant gut microbiota development. Nat. Commun. *7*, 11939.

van der Meer, J.R., and Belkin, S. (2010). Where microbiology meets microengineering: design and applications of reporter bacteria. Nat. Rev. Microbiol. *8*, 511–522.

Mizan, S., Henk, A., Stallings, A., Maier, M., and Lee, M.D. (2000). Cloning and characterization of sialidases with 2-6′ and 2-3′ sialyl lactose specificity from *Pasteurella multocida*. J. Bacteriol. *182*, 6874–6883.

Newburg, D.S., and Neubauer, S.H. (1995). Chapter 4. Carbohydrates in milks: analysis, quantities, and significance. In Handbook of Milk Composition, R.G. Jensen, ed. (Academic Press), pp. 273–349.

Newburg, D.S., Ruiz-Palacios, G.M., Altaye, M., Chaturvedi, P., Meinzen-Derr, J., Guerrero, M., de, L., and Morrow, A.L. (2004). Innate protection conferred by fucosylated oligosaccharides of human milk against diarrhea in breastfed infants. Glycobiology *14*, 253–263.

Newburg, D., Ko, J., Leone, S., and Nanthakumar, N.N. (2015). Human milk oligosaccharides and galactosyloligosaccharides attenuate inflammation in human intestine. FASEB J. *29*, Suppl, Abstract 252.1.

Packer, M.S., and Liu, D.R. (2015). Methods for the directed evolution of proteins. Nat. Rev. Genet. *16*, 379–394.

Paige, J.S., Nguyen-Duc, T., Song, W., and Jaffrey, S.R. (2012). Fluorescence imaging of cellular metabolites with RNA. Science *335*, 1194.

Paton, G.I., Reid, B.J., and Semple, K.T. (2009). Application of a luminescence-based biosensor for assessing naphthalene biodegradation in soils from a manufactured gas plant. Environ. Pollut. *157*, 1643–1648.

Petschacher, B., and Nidetzky, B. (2016). Biotechnological production of fucosylated human milk oligosaccharides: prokaryotic fucosyltransferases and their use in biocatalytic cascades or whole cell conversion systems. J. Biotechnol. *235*, 61–83.

Plante, O.J., Palmacci, E.R., and Seeberger, P.H. (2001). Automated solid-phase synthesis of oligosaccharides. Science *291*, 1523–1527.

Prudden, A.R., Liu, L., Capicciotti, C.J., Wolfert, M.A., Wang, S., Gao, Z., Meng, L., Moremen, K.W., and Boons, G.-J. (2017). Synthesis of asymmetrical multiantennary human milk oligosaccharides. Proc. Natl. Acad. Sci. USA *114*, 6954–6959.

Rinas, U., and Hoffmann, F. (2004). Selective leakage of host-cell proteins during high-cell-density cultivation of recombinant and non-recombinant *Escherichia coli*. Biotechnol. Prog. *20*, 679–687.

Royle, L. (2013). Chapter 8. Glycans and monosaccharides. Liquid Chromatography (Elsevier Science).

Rudd, P.M., Guile, G.R., Küster, B., Harvey, D.J., Opdenakker, G., and Dwek, R.A. (1997). Oligosaccharide sequencing technology. Nature *388*, 205–207.

Schwarz, F., Huang, W., Li, C., Schulz, B.L., Lizak, C., Palumbo, A., Numao, S., Neri, D., Aebi, M., and Wang, L.-X. (2010). A combined method for producing homogeneous glycoproteins with eukaryotic N-glycosylation. Nat. Chem. Biol. *6*, 264–266.

Sears, P., and Wong, C.H. (2001). Toward automated synthesis of oligosaccharides and glycoproteins. Science *291*, 2344–2350.

Sela, D.A., and Mills, D.A. (2010). Nursing our microbiota: molecular linkages between bifidobacteria and milk oligosaccharides. Trends Microbiol. *18*, 298–307.

Sela, D.A., Li, Y., Lerno, L., Wu, S., Marcobal, A.M., German, J.B., Chen, X., Lebrilla, C.B., and Mills, D.A. (2011). An infant-associated bacterial commensal utilizes breast milk sialyloligosaccharides. J. Biol. Chem. *286*, 11909–11918.

Sela, D.A., Garrido, D., Lerno, L., Wu, S., Tan, K., Eom, H.-J., Joachimiak, A., Lebrilla, C.B., and Mills, D.A. (2012). *Bifidobacterium longum* subsp. *infantis* ATCC 15697 α-fucosidases are active on fucosylated human milk oligosaccharides. Appl. Environ. Microbiol. *78*, 795–803.

Shen, Z., Warren, C.D., and Newburg, D.S. (2000). High-performance capillary electrophoresis of sialylated oligosaccharides of human milk. Anal. Biochem. *279*, 37–45.

Shis, D.L., and Bennett, M.R. (2013). Library of synthetic transcriptional AND gates built with split T7 RNA polymerase mutants. Proc. Natl. Acad. Sci. USA *110*, 5028–5033.

Shubhakar, A., Reiding, K.R., Gardner, R.A., Spencer, D.I.R., Fernandes, D.L., and Wuhrer, M. (2015). High-throughput analysis and automation for glycomics studies. Chromatographia *78*, 321–333.

Strack, R.L., Song, W., and Jaffrey, S.R. (2014). Using spinach-based sensors for fluorescence imaging of intracellular metabolites and proteins in living bacteria. Nat. Protoc. *9*, 146–155.

Suzuki, M., and Suzuki, A. (2001). Structural characterization of fucose-containing oligosaccharides by high-performance liquid chromatography and matrix-assisted laser desorption/ionization time-of-flight mass spectrometry. Biol. Chem. *382*, 251–257.

Thurl, S., Munzert, M., Henker, J., Boehm, G., Müller-Werner, B., Jelinek, J., and Stahl, B. (2010). Variation of human milk oligosaccharides in relation to milk groups and lactational periods. Br. J. Nutr. *104*, 1261–1271.

Trang, P.T.K., Berg, M., Viet, P.H., Van Mui, N., and Van Der Meer, J.R. (2005). Bacterial bioassay for rapid and accurate analysis of arsenic in highly variable groundwater samples. Environ. Sci. Technol. *39*, 7625–7630.

Underwood, M.A., Gaerlan, S., De Leoz, M.L.A., Dimapasoc, L., Kalanetra, K.M., Lemay, D.G., German, J.B., Mills, D.A., and Lebrilla, C.B. (2015). Human milk oligosaccharides in premature infants: absorption, excretion, and influence on the intestinal microbiota. Pediatr. Res. *78*, 670–677.

Valderrama-Rincon, J.D., Fisher, A.C., Merritt, J.H., Fan, Y.-Y., Reading, C.A., Chhiba, K., Heiss, C., Azadi, P., Aebi, M., and DeLisa, M.P. (2012). An engineered eukaryotic protein glycosylation pathway in *Escherichia coli*. Nat. Chem. Biol. *8*, 434–436.

Valentine, J.L., Chen, L., Perregaux, E.C., Weyant, K.B., Rosenthal, J.A., Heiss, C., Azadi, P., Fisher, A.C., Putnam, D., Moe, G.R., et al. (2016). Immunization with outer membrane vesicles displaying designer glycotopes yields class-switched, glycan-specific antibodies. Cell Chem. Biol. *23*, 655–665.

Wang, M., Li, M., Wu, S., Lebrilla, C.B., Chapkin, R.S., Ivanov, I., and Donovan, S.M. (2015). Fecal microbiota composition of breast-fed infants is correlated with human milk oligosaccharides consumed. J. Pediatr. Gastroenterol. Nutr. *60*, 825–833.

Ward, R.E., Niñonuevo, M., Mills, D.A., Lebrilla, C.B., and German, J.B. (2007). In vitro fermentability of human milk oligosaccharides by several strains of bifidobacteria. Mol. Nutr. Food Res. *51*, 1398–1405.

Xiao, Z., Guo, Y., Liu, Y., Li, L., Zhang, Q., Wen, L., Wang, X., Kondengaden, S.M., Wu, Z., Zhou, J., et al. (2016). Chemoenzymatic synthesis of a library of human milk oligosaccharides. J. Org. Chem. *81*, 5851–5865.

Yu, Z.-T., Nanthakumar, N.N., and Newburg, D.S. (2016). The human milk oligosaccharide 2′-fucosyllactose quenches *Campylobacter jejuni*-induced inflammation in human epithelial cells HEp-2 and HT-29 and in mouse intestinal mucosa. J. Nutr. *146*, 1980–1990.

Zhang, G., Brokx, S., and Weiner, J.H. (2006). Extracellular accumulation of recombinant proteins fused to the carrier protein YebF in *Escherichia coli*. Nat. Biotechnol. *24*, 100–104.

Zhao, C., Wu, Y., Yu, H., Shah, I.M., Li, Y., Zeng, J., Liu, B., Mills, D.A., and Chen, X. (2016). The one-pot multienzyme (OPME) synthesis of human blood group H antigens and a human milk oligosaccharide (HMOS) with highly active *Thermosynechococcus elongatus* α1-2-fucosyltransferase. Chem. Commun. *52*, 3899–3902.

Zhou, K., Qiao, K., Edgar, S., and Stephanopoulos, G. (2015). Distributing a metabolic pathway among a microbial consortium enhances production of natural products. Nat. Biotechnol. *33*, 377–383.

# STAR★METHODS

## KEY RESOURCES TABLE

| REAGENT or RESOURCE | SOURCE | IDENTIFIER |
|---|---|---|
| Bacterial and Virus Strains | | |
| NEB 5-alpha Competent *E.coli* | New England Biolabs | Catalog #C2987I |
| NEB 10-beta *E.coli* | New England Biolabs | Catalog #C3019I |
| BL21 (DE3) *E.coli* | New England Biolabs | Catalog #C2527I |
| Bifidobacterium longum subsp. infantis | American Type Culture Collection | ATCC #15697D-5 |
| JM109 gwBC-F2 | Gift from Georg Sprenger (Baumgärtner et al., 2013) | N/A |
| JM109 gwBC | Gift from Georg Sprenger (Baumgärtner et al., 2013) | N/A |
| Chemicals, Peptides, and Recombinant Proteins | | |
| 2'-Fucosyllactose | Carbosynth | CAS #41263-94-9 |
| 3-Fucosyllactose | Carbosynth | CAS #41312-47-4 |
| 3'-Sialyllactose sodium salt | Carbosynth | CAS #128596-80-5 |
| 6'-Sialyllactose sodium salt | Carbosynth | CAS #157574-76-0 |
| Lacto-N-triose II | Carbosynth | CAS #75645-27-1 |
| 2-chloro-4-nitrophenyl-α-L-fucopyranoside | Carbosynth | CAS #157843-41-9 |
| Critical Commercial Assays | | |
| Neuraminidase Assay Kit | Sigma-Aldrich | MAK121-1KT |
| L-Fucose Assay Kit | Megazyme | K-FUCOSE |
| Oligonucleotides | | |
| See Table S3 | Iowa State University DNA Facility | N/A |
| Recombinant DNA | | |
| pET28:GFP | Gift from Matthew Bennett (Shis and Bennett, 2013) | Addgene Plasmid #60733 |
| pHL 1277 | Gift from Han Lim (Hung et al., 2014) | Addgene Plasmid #53017 |
| pET28:mCherry | This manuscript | N/A |
| pAfcA | Gen9 | N/A |
| pAfcB | This manuscript | N/A |
| pNanH | Gen9 | N/A |
| pNanH2 | This manuscript | N/A |
| pYebF-NanH2 | This manuscript | N/A |
| pBnaG | Gen9 | N/A |
| Software and Algorithms | | |
| SAS version 9.4 | SAS institute | https://www.sas.com/en_us/home.html |

## CONTACT FOR REAGENT AND RESOURCE SHARING

Further information and requests for resources and reagents should be directed to and will be fulfilled by the Lead Contact, Thomas J. Mansell (mansell@iastate.edu)

## EXPERIMENTAL MODEL AND SUBJECT DETAILS

### Bacterial Strains and Plasmids

The plasmids and strains used in this study are listed in Table 1. *E. coli* NEB 5-alpha (New England Biolabs Inc., Ipswich, MA) were used for routine cloning and *E. coli* BL21 (DE3) was used for oligosaccharide detection and growth experiments. The plasmid

pET28:GFP was a gift from Matthew Bennett (Addgene plasmid # 60733). pET28:GFP is the pET28b expression vector with GFP downstream of the T7-specific promoter PT7/LacO, which contains binding sites for the lactose repressor, LacI (Shis and Bennett, 2013). Plasmid pET28:mCherry was constructed via Gibson Assembly using mCherry DNA amplified from plasmid pHL1277. The plasmid pHL 1277 was a gift from Han Lim (Addgene plasmid # 53017) (Hung et al., 2014).

Plasmid pAfcA was constructed by DNA synthesis of an operon comprising a promoter, ribosome binding site, signal sequence, and glycosidase open reading frame which was cloned into plasmid pG9m-2 by Gen9 (Cambridge, MA). Promoter J23110 from the Anderson promoter collection and Shine-Dalgarno sequence (BBa_J34801) were chosen as a strong constitutive promoter and ribosome binding site from the Registry of Standard Biological Parts (http://parts.igem.org). To facilitate periplasmic export of the glycosidase, the 22 amino acid signal sequence of *pelB* from *Dickeya dadantii* was encoded immediately upstream of the 1,2-α-L-fucosidase domain (residues 577-1,474) of gene *afcA* from *Bifidobacterium bifidum*, which was codon-optimized for *E. coli* (IDT DNA Codon Optimization Tool). Plasmid pAfcB was constructed by replacement of the *afcA* fucosidase domain with the 1,3-α-L-fucosidase domain (residues 19-471) of the *afcB* gene. This gene was amplified by PCR from the genomic DNA of *Bifidobacterium longum subsp. infantis* ATCC 15697™ (American Type Culture Collection, Manassas, VA). The afcB fragment was assembled into the same vector using NEBuilder® HiFi DNA Assembly Master Mix (New England Biolabs Inc., Ipswich, MA) with the amplicons digested with DpnI before PCR purification. The genes encoding NanH (*P. multocida*) and BnaG (*L. casei*) were similarly synthesized by Gen9 (residues 29-778 and 32-533 respectively). The gene encoding NanH2 (*B. longum sp. infantis*), composed of 394 residues, was amplified from genomic DNA (ATCC 15697) and cloned into pAfcA using NEB Hifi Assembly. The oligonucleotide primers for the construction of the plasmids are listed in Table S3. The gene sequences of the constructs can be found in the Data S1.

### Cell Culture and Induction

Competent BL21 (DE3) cells were co-transformed with pET28:GFP and either pAfcA, pAfcB, pNanH, pNanH2 or pBnaG by electroporation. After transformation and recovery, single colonies of the transformed cells were grown in Luria-Bertani (LB) media (1% tryptone, 0.5% yeast extract, and 1% NaCl) containing appropriate antibiotics at 37°C in a shaking incubator. Media was supplemented with antibiotics at the following final concentrations: 50 μg $ml^{-1}$ carbenicillin and/or 30 μg $ml^{-1}$ kanamycin. Cells were grown to mid-exponential phase ($OD_{600}$ of approximately 0.6) before addition of carbohydrate inducer. Cultures were induced by adding 2'-FL, and 3-FL to a final concentration of 0.3% or 3'-SL and 6'-SL to a final concentration of 0.4% or lacto-N-triose II to a final concentration of 0.32%. All oligosaccharides were sourced from Carbosynth (Carbosynth, Berkshire, UK). Isopropyl β-D-1-thiogalactopyranoside (IPTG; Invitrogen, Carlsbad, CA) and lactose were added to a final concentration of 0.1mM and 0.2% respectively. All oligosaccharide concentrations are molar equivalents to 0.2% lactose. These cultures were then incubated at 37 °C in a rotary shaker (250 rpm) for 16 hr. In cultures with supplemented exogenous fucosidase, 0.012 Units of α-1,2-fucosidase (Megazyme) were added to growth media before induction.

## METHOD DETAILS

### Measurement of GFP Fluorescence

To quantify the green fluorescence intensity of the GFP, 150 μL of the overnight culture of GFP expressing bacterial cells was harvested, washed and re-suspended in 500 μL 1X PBS (phosphate buffered saline). Standard curves were prepared in the range from 0 mg/L to 3000 mg/L. Expression data of the resuspended cells were collected the Iowa State Flow Cytometry Facility (Ames, IA) using a BD FACSCanto Plus RUO (San Jose, CA) flow cytometer with a solid state 488 nm/20 mW (nanometer/milliWatt) blue laser and a 505 nm-long pass and 525/50 nm-band pass filter set. Cells were gated for forward and side scatter to avoid aggregated cells and debris. All measurements of fluorescence were obtained from three independent biological replicates maintained under identical conditions. For each culture, 25,000-40,000 events were collected.

### Production of 2'-FL

The 2'-FL producing strain, JM109 gwBC-F2, obtained from G. Sprenger (Universität Stuttgart) was cultivated in a shake flask. JM109 gwBC strain without fucosyltransferase *futC* genes was used as control. The shake flask experiments were carried out in 1 L shake flasks with 250 mL minimal media and 1% glycerol as the carbon source, according to the protocol listed in the paper (Baumgärtner et al., 2013). At mid log phase, IPTG (0.5 mM) and lactose (2%) were added and the cultures were grown for 24 h before pelleting and washing them. All culture and growth conditions for the control were identical to the 2'-FL producing strain. Cell lysis was carried out by sonication. Oligosaccharide concentrations in the lysates were determined by LC-MS before testing with the biosensor. Serial dilutions of 30% commercial 2'-FL with added lysate from the non 2'-FL producing strain, was used to generate a calibration curve for absolute quantitation of 2'-FL in the lysate (Figure S1D). The same volume of control lysate was added as the 2'-FL producing strain lysate. The run order of samples was randomized to ensure that any biological variation is independent of systematic bias in the analytical process.

### Validation with LC-MS

2'-FL concentrations from cell lysates were verified by HPLC-MS. HPLC analysis was performed on Agilent Technologies 1100 Series HPLC system coupled to an Agilent Technologies Mass Selective Trap SL detector (Agilent Technologies, Santa Clara,

CA) equipped with an electrospray ion source (ESI) and controlled by ChemStation A.10.02, including data acquisition and processing. Products were analyzed on a Luna C18 reversed phase column (150 mm× 2 mm, 5 μm, Phenomenex, Germany) detected by electrospray ionization (positive ion mode). Mobile phase consisted of solvent 1 (aqueous solution containing formic acid 0.1% (v/v)) and solvent 2 (acetonitrile containing formic acid 0.1% (v/v)). The LC gradient was delivered at 0.4 ml/min, and consisted of an initial linear increase from 100% solvent 1/0% solvent 2 to 0% solvent 1/100% solvent 2 over 15 min, followed by a linear decrease to starting conditions for 5 min, allowing a sample injection every 30 minutes. 5 μL of sample was injected and the column temperature kept at 40°C. Standards and samples were analyzed in triplicates and standard curves were created from six different concentrations. Identification of 2'-FL by mass spectrometry was completed by comparison with 2'-FL standard (Figure S1C).

### Growth of Strain with a Sole Carbon Source

Cells were cultured in M9 minimal media (M9 salts, $MgSO_4$, $CaCl_2$ and 0.1% thiamine) which was supplemented with glucose, lactose, 2'-FL or 3-FL. 200 μL of the media was inoculated with cells in mid-log phase after the cells were washed with the minimal media in a clear bottom 96-well plate (Corning). The growth of the cells was monitored by measuring the optical density at 600 nm at 37°C on a Synergy neo2 plate reader (BioTek, Winooski, VT).

### Coculture Experiments in Defined Media

Single colonies harboring pAfcA and pAfcB were picked from agar plates and incubated with 5 mL of LB at 37°C. The cells were cultivated at 37°C to mid-log phase, washed with distilled water and inoculated at 1 % into 300 μL of M9 minimal media supplemented with 2 mM MgSO4, 0.1 mM CaCl2 and 0.1% thiamine at ratios of 1:1, 1:10, and 1:100 with a single carbon source: lactose, 2'-FL or 3-FL and allowed to grow for 72 hr. After enrichment, cells from the co-culture were then diluted and plated on agar plates and incubated at 37°C overnight. Thirty to fifty of the single colonies were randomly selected and subjected to multiplex colony PCR with primers corresponding to *afcA* and *afcB* to determine the proportion of specific plasmids in the mixed population. For colony PCR, OneTaq 2x Master Mix (New England Biolabs Inc., Ipswich, MA) were used according to the protocols supplied by the manufacturer. The products were visualized in agarose gels. All enrichments were cultured in triplicate.

The GFP/RFP reporter assays were conducted in the same way with a coculture at 1:1 ratio in a defined media with a single carbohydrate source and the fluorescence analyzed on a plate reader (200 μL in each well). The plate was sealed with a Breathe Easy sealing membrane (Millipore Sigma, St. Louis, MO) and subjected to continuous orbital shaking. Measurements were made every 10 minutes. Once the cells reached their stationary phase, the cells were pelleted and washed twice in PBS before inoculating at 0.1% into fresh media with the second carbohydrate source. This was repeated for another cycle and reverting to the first carbohydrate source. Excitation and emission wavelengths were 485 nm and 528 nm respectively for GFP and 590 nm and 645 nm for mCherry respectively. Statistical analysis was done using SAS (version 9.4; SAS Institute Inc, Cary, NC). The proportions of cells expressing either plasmid were modeled using a binomial distribution with the replicates as the random variable and the carbon source, starting inoculation ratio and respective genes as independent variables. Statistical significance was set at $P < 0.0001$ for all analyses. To determine crosstalk between the two strains, the experiments were carried out identically, but in LB with a single carbohydrate source.

### Selective Lactose Removal

Cells harboring pAfcA were grown to mid-log phase in LB. The inocula were supplemented with lactose (0.2%) or 2'-FL (0.3%) and varying levels of β-galactosidase (Millipore Sigma, St. Louis, MO). The β-galactosidase was reconstituted by dissolving in 1 mM magnesium chloride. Here, one unit hydrolyzes 1.0 μmole of o-nitrophenyl β-D-galactoside to o-nitrophenol and D-galactose per minute. The cultures were grown overnight at 37 °C and analyzed on a flow cytometer.

For pre-treatment with cells that consume lactose, BL21 (DE3) cells were grown to mid-log phase in LB and spiked with equimolar lactose (0.003%), 2'-FL (0.005%) or a mixture of lactose and 2'-FL. After incubating for 1, 2 or 3h, they were spun down and the supernatant added to the biosensing cells. These cultures were similarly analyzed on a flow cytometer. For lactose precipitation and cell lysis with ethanol, two volumes of ethanol were added to the culture and incubated for 4 h before being spun down and the supernatant collected. This lysate was incubated overnight at 4 °C and the precipitated lactose was removed by filtration. Different concentrations of lysate were added to a final volume of 300 μL. The final ethanol concentrations in the cultures ranged from 0 to 2% (v/v), not considering the losses due to evaporation.

### Enzymatic Assays

To quantify the α-2,3-sialidase enzymes, a commercial enzymatic assay was carried out on supernatant and lysates of NanH and NanH2 biosensing cells. The sialidase activity was measured using Neuraminidase Assay Kit (Sigma-Aldrich, St. Louis, MO) according to the protocols supplied by the manufacturer. The samples were diluted 100-fold before testing. One unit of neuraminidase activity was defined as the amount of enzyme that generates 1.0 μmol of sialic acid per minute at pH 7.4 at 37°C.

To quantify the α-1,2-L-fucosidase and α-1,3-L-fucosidase, 5 mL of pAfcA/pAfcB expressing cells were grown in LB, washed and concentrated ten-fold before lysing via sonication. The pAfcA lysate was incubated with varying concentrations of 2'-FL in 10 mM sodium phosphate buffer (pH 7.0) at 30°C. The reaction mixtures were boiled for 3 minutes before using the L-Fucose Assay Kit (Megazyme) to determine the amount of fucose released. One unit of α-1,2-L-fucosidase activity was defined as the amount of enzyme required to release one μmol of α-L-fucose per minute from 2'-FL (2 mM) in sodium phosphate buffer (10 mM), pH 7 at

30°C. The pAfcB lysate was incubated with varying concentrations of 2-chloro-4-nitrophenyl-α-L-fucopyranoside (CNP-fucose; Carbosynth, Berkshire, UK) in McIlvaine buffer, pH 5.6 (citric acid/disodium hydrogen phosphate) at 37°C for 10 minutes and the reactions were stopped by addition of 1 M $Na_2CO_3$. Absorbance at 405 nm was measured on a Synergy neo2 plate reader (BioTek, Winooski, VT). One unit of α-1,3-L-fucosidase activity was defined as the amount of enzyme required to hydrolyze one μmol of CNP-fucose to 2-chloro-4-nitrophenol per minute in McIlvaine buffer, pH 6 at 37°C. All enzyme concentrations in μM were estimated by calculation of the $[E]_{total}$ from $V_{max}$ using cited Michaelis-Menten parameters with respect to the observed velocity in the assay of interest.

## QUANTIFICATION AND STATISTICAL ANALYSIS

Non-linear regression was used for statistical analysis and the calibration curve was analyzed using the Four Parameter Logistic (4PL) model:

$$y = d + \frac{(a - d)}{1 + \left(\frac{x}{c}\right)^{b}}$$

where: $a$ = Minimum asymptote representing minimum reporter activity; $b$ = Hill's slope; $c$ = Inflection midpoint, or the concentration of analyte where $y=(d-a)/2$, representative of the position of linear region; $d$ = Maximum asymptote representing maximum reporter activity.

MATLAB (MathWorks, Natick, MA) was used to fit the 4PL model using the built-in *fit* function to determine estimates of the parameters using a nonlinear least-squares method.

All statistical analysis and associated error bars have been identified in the figure captions.

## DATA AND SOFTWARE AVAILABILITY

All DNA sequences of genes used for this study are contained in Data S1. Representative LC-MS runs and standard curves appear in Figure S2 but raw LC-MS data are available upon request.